

## Controlling the Scattering Length of Ultracold Dipolar Molecules

Lucas Lassablière and Goulven Quéméner

*Laboratoire Aimé Cotton, CNRS, Université Paris-Sud, ENS Paris-Saclay, Université Paris-Saclay, 91405 Orsay, France*

 (Received 22 June 2018; published 16 October 2018)

By applying a circularly polarized and slightly blue-detuned microwave field with respect to the first excited rotational state of a dipolar molecule, one can engineer a long-range, shallow potential well in the entrance channel of the two colliding partners. As the applied microwave ac field is increased, the long-range well becomes deeper and can support a certain number of bound states, which in turn bring the value of the molecule-molecule scattering length from a large negative value to a large positive one. We adopt an adimensional approach where the molecules are described by a rescaled rotational constant  $\tilde{B} = B/s_{E_3}$  where  $s_{E_3}$  is a characteristic dipolar energy. We found that molecules with  $\tilde{B} > 10^8$  are immune to any quenching losses when a sufficient ac field is applied, the ratio elastic to quenching processes can reach values above  $10^3$ , and that the value and sign of the scattering length can be tuned. The ability to control the molecular scattering length opens the door for a rich, strongly correlated, many-body physics for ultracold molecules, similar to that for ultracold atoms.

DOI: 10.1103/PhysRevLett.121.163402

Controlling the scattering length  $a$  between ultracold particles is at the center of most modern ultracold gases experiments. The scattering length corresponds to an effective parameter that characterizes the range of the particles interaction at ultralow energy. The value and the sign of the scattering length control the interaction strength and stability of such gases [1,2]. A weakly interacting gas is defined when the scattering length  $a$  is much smaller than the mean relative distance  $\bar{d}$  between the particles,  $|a|/\bar{d} \ll 1$ . In contrast, a strongly interacting gas is defined when  $|a|/\bar{d} \gg 1$  and leads to a strong correlated state of matter [3,4]. In the unitary regime, the scattering length diverges to an infinite value, positive or negative. With fermionic particles, the strongly interacting regime represents a cross over between the BEC to the BCS weakly interacting regimes, when the very large scattering length changes sign from positive to negative [5–8]. With bosonic particles, few-body physics becomes strongly universal [9] as underlined by the Efimov effect [10,11]. Finally, controlling the scattering length of particles in optical lattices is very important to engineering tunable many-body Hamiltonians, to simulate untractable systems of condensed matter [12,13].

In experiments of ultracold atoms, the control of the scattering length is usually possible in the vicinity of a Fano-Feshbach resonance [14,15] when a magnetic field [16–18] or an optical electromagnetic field [19–21] is tuned to an appropriate value. However, in experiments of ultracold molecules, for example ultracold alkali dipolar molecules [22–28], finding a well-resolved, isolated Fano-Feshbach resonance is a difficult task because of the very high density of states of tetramer bound states in the vicinity of the low-energy collisional threshold [29,30].

Even worse, this very high density of states yields long-lived tetramer complexes explaining losses in elastic collisions of nonreactive molecules [31]. Therefore, the ability to tune the scattering length seems compromised for molecules.

In this Letter, we show how we can control the molecule-molecule scattering length, which in this case becomes a complex quantity  $a = a_{\text{re}} - ia_{\text{im}}$  with  $a_{\text{im}} \geq 0$  [32,33]. By applying a microwave field slightly blue-detuned with respect to the first excited rotational state of the molecule, one can (i) bring the ratio good to bad collisions  $\gamma = \beta_{\text{el}}/\beta_{\text{qu}}$  (elastic over quenching rate coefficient) to high values such that evaporative cooling techniques can be successful; (ii) suppress the imaginary part  $a_{\text{im}} \rightarrow 0$  and shield the molecules against losses; (iii) tune the real part  $a_{\text{re}}$  to small or large values, positive or negative (hence,

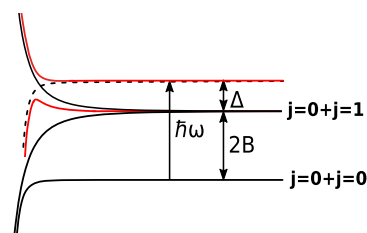


FIG. 1. Schematic process of a collisional shielding of ground state rotational molecules  $j = 0$ , using a blue-detuned, circularly polarized microwave field.  $\Delta > 0$  is the detuning between the energy of the microwave field  $\hbar\omega$  and  $2B$ , the energy level of the first excited rotational state  $j = 1$  of a molecule. The dipole-dipole interaction creates an effective repulsive adiabatic curve (plotted in red), preventing the molecules from approaching at short range.

tune the value of the elastic cross section  $\sigma_{el}$ ) and control the interaction strength of an ultracold molecular gas. By tuning in this way, the scattering length at will, one can access with ultracold molecules the same rich and flexible, strongly correlated many-body physics of ultracold atoms as mentioned above. The basis of the method comes from the idea of optical shielding [34–37]. The schematic process is illustrated in Fig. 1. Instead of having an optical transition slightly blue-detuned between an  $s$  to a  $p$  electronic state of an atom, one has a microwave transition of energy  $\hbar\omega$  [38–40] between a  $j = 0$  to a  $j = 1$  rotational state of energy  $2B$ , where  $B$  is the rotational constant of the molecule. The detuning is given by  $\Delta = \hbar\omega - 2B > 0$ . For the shielding to take place, it is important for the polarization of the microwave to be circular [36].

We consider bosonic  $^1\Sigma^+$  alkali dipolar molecules in the vibrational state  $v = 0$  with a permanent electric dipole moment  $d$ . This study can be generalized to fermionic ones. To describe the collisions between ultracold molecules, we use a time-independent quantum formalism [41–43] including the rotational structure of the molecules described by a properly symmetrized and normalized basis set  $|j_1 m_{j_1}, j_2 m_{j_2}\rangle_{\pm}$ , symmetric (+) or antisymmetric (–) under permutation of the identical molecules. We include the rotational states  $j_1 = 0, 1$  and  $j_2 = 0, 1$ . Additionally, a partial wave expansion of the collisional wave function described by a spherical harmonics basis set  $|lm_l\rangle$  is used. The partial waves taken into account are  $l = 0, 2, 4$ . We only include a long-range dipole-dipole interaction and an isotropic, electronic van der Waals coefficient [43]. We also impose that when the two molecules come close to each other at short range, they are lost with a unit probability [41–43]. These assumptions are sufficient to reproduce available experimental data of either reactive [44,45] or nonreactive [31] ultracold molecular collisions. We numerically solve a set of close-coupled Schrödinger equations and by applying asymptotic boundary conditions, we extract the scattering matrix  $S$  from which we can deduce the scattering length and the experimental observables such as the cross sections and the rate coefficients [41]. The complex scattering length  $a$  is related to the lowest entrance channel scattering matrix element  $S_{00}$  [33] by:  $a = \lim_{k \rightarrow 0} (1/ik) \{ [1 - S_{00}(k)] / [1 + S_{00}(k)] \}$ ,

where  $k = \sqrt{2\mu E_c / \hbar^2}$  is the wave vector,  $E_c$  the collision energy and  $\mu$  the reduced mass between the two molecules. To include the electromagnetic field, we employ a quantized formalism of the field, described by a basis  $|\bar{n} + n\rangle$  (see Refs. [36,46,47] for more details). This corresponds to the number of photons in the quantized field reservoir for a given mode  $\hbar\omega$ , with  $|n| \ll \bar{n}$ .  $\bar{n}$  is a mean number (and is omitted hereafter in the notation),  $n$  represents the number of photon lost from the quantized field and absorbed by the molecule if  $n < 0$  or gained by the quantized field and emitted by the molecule if  $n > 0$ . In the numerical calculation, we consider  $n = 0, \pm 1, \pm 2$ . As for the optical shielding to take place, we consider a blue-detuned

microwave with respect to the first rotational excited state of the molecules, with a  $\sigma^+$  circular polarization characterized by a quantum number  $p = +1$  [36,46,47].

As many experimental groups are now forming different ultracold dipolar alkali molecules, we do not restrict our study to a specific system and rather employ a general, adimensional approach to treat the molecules on the same basis. We study the microwave shielding and the control of the scattering length of all possible molecules described by their combined values of  $B$ ,  $d$ , and  $\mu$  as a function of the ac field  $E_{ac}$  of the microwave for a fixed detuning  $\Delta$ . Simultaneously and independently, a recent study [40] explored the microwave shielding as a function of  $E_{ac}$  and  $\Delta$  for three specific molecules RbCs, KCs, and CaF. In their work, they also explored the effect of the hyperfine structure on the shielding mechanism. We do not include the hyperfine structure to keep our study adimensional. Following the conclusions of Ref. [40], the assumption is valid as far as the hyperfine quantum numbers are nearly good quantum numbers and decoupled from the rotational structure when a sufficient magnetic field is applied (see also Ref. [48]). We employ the same adimensional approach as our previous study on shielding ultracold dipolar molecules in an electric dc field [43]. Here, the dc field is replaced by the ac field  $E_{ac}$ . We rescale the Schrödinger equation using the characteristic dipolar length  $s_{r_3} = (2\mu/\hbar^2)(d^2/4\pi\epsilon_0)$  and the characteristic dipolar energy  $s_{E_3} = (\hbar^2/2\mu s_{r_3}^2)$  [75]. The values are reported in the table in Ref. [48]. We then extract four key parameters in the set of close-coupling rescaled Schrödinger equations very similar to the ones in our previous dc field study. The first parameter is a rescaled rotational constant

$$\tilde{B} = \frac{B}{s_{E_3}} = \frac{8B\mu^3}{\hbar^6} \left( \frac{d^2}{4\pi\epsilon_0} \right)^2. \quad (1)$$

Another parameter is a rescaled ac field  $\tilde{E}_{ac} = dE_{ac}/B$ . From the usual expression of the Rabi frequency  $\Omega = dE_{ac}/\hbar$ , one can define a rescaled Rabi frequency:

$$\tilde{\Omega} = \frac{\Omega}{B/\hbar} = \frac{dE_{ac}}{B} \equiv \tilde{E}_{ac} \quad (2)$$

which becomes the second parameter and identifies with the rescaled ac field. A third parameter corresponds to a rescaled detuning:

$$\tilde{\Delta} = \frac{\Delta}{B} = \frac{\hbar\omega - 2B}{B}. \quad (3)$$

In this study, we fix this third parameter to an arbitrary positive constant of  $\tilde{\Delta} = 0.025$  (blue-detuned). We choose the values of  $\tilde{\Delta}$  and  $\tilde{\Omega}$  appropriately so that the blue-detuned microwave radiation does not lead to an antitrapping effect of the molecules (see Ref. [48]).

Finally, the fourth parameter is a rescaled collision energy  $\tilde{E}_c = E_c/s_{E_3}$ . To get rid of the collision energy dependence in our study, we consider the Wigner regime as  $E_c \rightarrow 0$  and where the scattering length is independent of the collision energy. The adimensional study entails a rescaled scattering length:

$$\tilde{a} = \tilde{a}_{\text{re}} - i\tilde{a}_{\text{im}} = \frac{a}{s_{r_3}}. \quad (4)$$

The ratio  $\gamma$  of the elastic over the quenching rate coefficient (see Ref. [43]) is given in terms of the rescaled scattering length by  $\gamma = (\beta_{\text{el}}/\beta_{\text{qu}}) = (|a|^2/a_{\text{im}})k = (|\tilde{a}|^2/\tilde{a}_{\text{im}})\tilde{k}$ , where  $\tilde{k} = \sqrt{\tilde{E}_c} = \sqrt{E_c/s_{E_3}}$ .

We consider molecules initially prepared in their ground rotational state  $|00, 00\rangle_+$  and  $|n = 0\rangle$ . Only the symmetric states exist for same, indistinguishable states and are coupled to other symmetric states. The quantum states  $|j_1 m_{j_1}, j_2 m_{j_2}\rangle_+ |n\rangle$  get mixed by the interaction of the molecules with the ac field [36,46,47] and give rise to dressed asymptotic states, denoted  $\{|j_1 m_{j_1}, j_2 m_{j_2}\rangle_+ |n\rangle\}$ . This notation means that they tend to the undressed state  $|j_1 m_{j_1}, j_2 m_{j_2}\rangle_+ |n\rangle$  when  $\tilde{\Omega} \rightarrow 0$ . We use a dressed state formalism, as the typical microwave Rabi oscillations times in this study are much smaller than the other characteristic times (see Ref. [48]). These states are characterized by well-defined projection numbers  $m_{\text{mol}_1 + \text{mol}_2 + \text{field}} = m_{j_1} + m_{j_2} + n \times p$  (with  $n, p$  being signed integer numbers) of the dressed system {molecule 1 + molecule 2 + field}. The dipole-dipole interaction will further couple the collisional states  $\{|j_1 m_{j_1}, j_2 m_{j_2}\rangle_+ |n\rangle\} |l m_l\rangle$  all together. The total projection number  $M = m_{\text{mol}_1 + \text{mol}_2 + \text{field}} + m_l$  is conserved during the collision. For the study of the scattering length at ultralow energies and given our initial state with  $m_{\text{mol}_1 + \text{mol}_2 + \text{field}} = 0$ , we consider the lowest projection  $M = 0$ , which implies  $m_l = 0$ .

The dipole-dipole couplings result in adiabatic effective potentials illustrated in Fig. 2(a) as a function of the rescaled distance  $\tilde{r} = r/s_{r_3}$  between the molecules, for an example at  $\tilde{B} = 10^{10}$  and  $\tilde{\Omega} = 0.18$ . Strong repulsive curves arise in the initial entrance channel  $\{|00, 00\rangle_+ |0\rangle\}$  indicated by an arrow, explaining more quantitatively the scheme in Fig. 1. This prevents the molecules from coming close to each other and being lost from chemical reactions [44,45] or from long-lived tetramer complexes [31] at short range. In addition, states of lower energy exist, corresponding to the excitation of one (resp. both) of the molecules in a specific  $j, m_j$  state due to the absorption of one (resp. two) photon lost by the quantized field with  $n = -1$  (resp.  $n = -2$ ). When  $\tilde{\Omega}$  is increased, these states get far away from the entrance channel thus preventing inelastic transitions from occurring. The quenching collisions (short-range losses + inelastic processes) are expected to be suppressed with  $\tilde{\Omega}$ , explaining the mechanism of the microwave shielding.

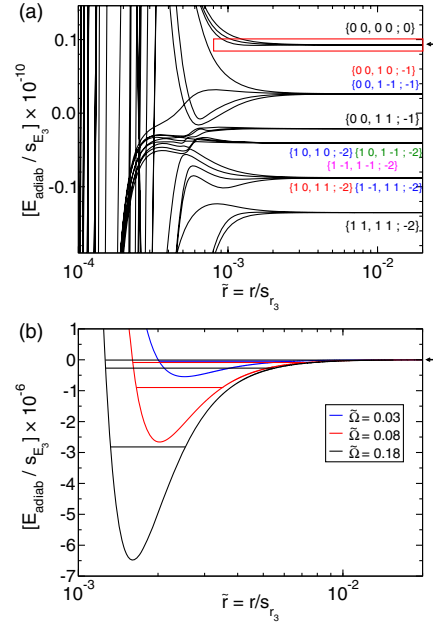


FIG. 2. (a) Top panel: Long-range rescaled adiabatic energies as a function of the rescaled distance between the molecules for  $\tilde{B} = 10^{10}$ ,  $\tilde{\Omega} = 0.18$ , and  $\sigma^+$  circularly polarized field  $p = +1$ . The region in the red box is shown in the bottom panel. The notation  $\{j_1 m_{j_1}, j_2 m_{j_2}; n\}$  is used to represent the asymptotic dressed states. The labels in black (resp. red, blue, green, magenta) correspond to values of  $m_{\text{mol}_1 + \text{mol}_2 + \text{field}} = m_{j_1} + m_{j_2} + n \times p = 0$  (resp.  $-1, -2, -3, -4$ ) of the dressed system {molecule 1 + molecule 2 + field}. (b) Bottom panel: Close-up of the long-range potential well in the lowest entrance channel for  $\tilde{B} = 10^{10}$  and  $\tilde{\Omega} = 0.18$  (black),  $\tilde{\Omega} = 0.08$  (red),  $\tilde{\Omega} = 0.03$  (blue) together with the corresponding bound state energies they can support.

In Fig. 3, we present the quantity  $|\tilde{a}|^2/\tilde{a}_{\text{im}}$  which represents the ratio  $\gamma$  when  $\tilde{k} = 1$ , that is at a typical collision energy of  $E_c = s_{E_3}$ . To get the ratio at  $E_c > s_{E_3}$ , one has to multiply this quantity by  $\tilde{k}$ . For evaporative

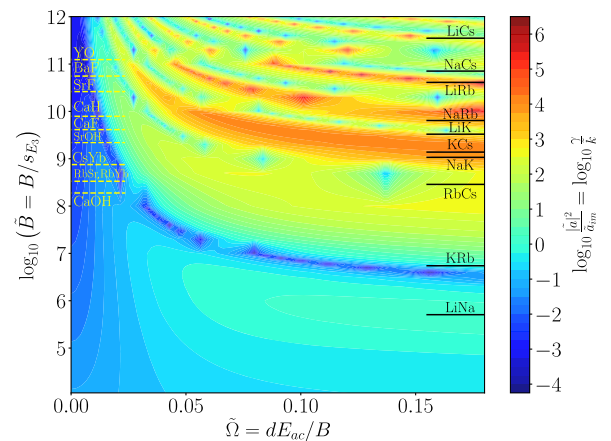


FIG. 3.  $|\tilde{a}|^2/\tilde{a}_{\text{im}} \equiv \gamma/\tilde{k}$  as a function of  $\tilde{B}$  and  $\tilde{\Omega}$ . The color scale, presented at the right of the picture, goes from  $10^{-4}$  to  $10^6$ . The  $\tilde{B}$  values of some characteristic dipolar molecules are reported on the figure.

cooling techniques,  $\gamma$  has to reach a factor of  $10^3$  or more for the process to be highly efficient. Therefore, the regions of the graph in yellow, orange, and red correspond to favorable conditions for evaporative cooling. The regions in green and blue correspond to unfavorable conditions. The rescaled Rabi frequency is plotted in the abscissa and represents the amount of the ac field applied. The rescaled rotational constant is plotted in ordinate and uniquely characterizes a molecule (see Table in Ref. [48]). The values of the dipolar alkali molecules have been reported. For indication, we also report values for  ${}^2\Sigma^+$  molecules of current experimental interest [76–88]. Looking at the general feature of the figure, one can distinguish two main regions for the dipolar molecules: a region for which  $\tilde{B} > 10^8$  where the ratio can globally reach  $10^3$  or more, and a region for which  $\tilde{B} < 10^7$  where the ratio barely reach  $10^2$ . The former region includes the molecules RbCs, NaK, KCs, LiK, NaRb, LiRb, NaCs, LiCs and determines the good candidates for the microwave shielding. This figure also confirms the suppressed loss rates found for the RbCs and KCs molecules [40]. The latter region includes the molecules KRb and LiNa for which the microwave shielding will not be efficient for the present range of  $\tilde{\Omega}$ . This is due to an unfortunate combination of  $\mu$ ,  $d$ , and  $B$  yielding a too low value of  $\tilde{B}$ .

In Fig. 4(a), we plot  $\tilde{a}_{\text{re}}$  and  $\tilde{a}_{\text{im}}$  as a function of  $\tilde{\Omega}$  for a value  $\tilde{B} = 10^{10}$  ( $\sim$ NaRb). There are values of  $\tilde{\Omega}$ , hence, of the ac field, for which the real part  $\tilde{a}_{\text{re}}$  can take large positive and negative values while the

imaginary part  $\tilde{a}_{\text{im}}$  remains low. Then, the elastic cross sections which are proportional to  $\tilde{a}_{\text{re}}$  [43] if  $a_{\text{im}} \rightarrow 0$  can be tuned to any desired values up to the maximal value given by the unitarity limit  $2 \times \pi/k^2$  for indistinguishable molecules. The imaginary part globally decreases when  $\tilde{\Omega}$  increases, confirming that the quenching rate coefficients, which are proportional to  $\tilde{a}_{\text{im}}$  [43], also decreases as expected from the discussion of the adiabatic curves in Fig. 2(a). The resonant features are explained by the apparition of a long-range, isolated shallow potential well in the entrance channel when  $\tilde{\Omega}$  is increased. This is illustrated in Fig. 2(b) which is a close-up of the lowest entrance channel of Fig. 2(a). At  $\tilde{\Omega} = 0.18$  (black curve), the well can support three bound states shown on the figure. If  $\tilde{\Omega}$  is decreased, the depth of the well also decreases and those bound states can disappear. For example, down at  $\tilde{\Omega} = 0.08$  (red curve), the well supports now only two bound states and at  $\tilde{\Omega} = 0.03$  (blue curve), it supports only one. When the bound states are localized at the zero energy threshold, typically for values of  $\tilde{\Omega}$  slightly below 0.18, 0.08, and 0.03,  $\tilde{a}_{\text{re}}$  turns from a large and positive value to a large and negative value, as seen in Fig. 4(a).

We present in Fig. 4(b) the trend of the scattering length for increasing values of  $\tilde{B} = 10^7, 10^9, 10^{11}$ . For a small value of  $\tilde{B} = 10^7$  ( $\sim$ KRb, black curves), one cannot see any resonant features of  $\tilde{a}$  for the present range of  $\tilde{\Omega}$ . When  $\tilde{B}$  is increased, typically for  $\tilde{B} \geq 10^8$ , the long-range wells are deep enough to support bound states, and resonant features appear in the scattering length as in Fig. 4(a). This is shown for  $\tilde{B} = 10^9$  ( $\sim$ NaK, KCs, red curves) and  $\tilde{B} = 10^{11}$  ( $\sim$ NaCs, blue curves). These long-range bound states are actually reminiscent of the so-called field-linked states [89,90] in collisions of dipolar molecules in a static electric field. The presence of these microwave field-linked states in the long-range wells, when the condition  $\tilde{B} \geq 10^8$  is satisfied, is therefore responsible for the control of the scattering length of dipolar molecules.

Technological set-ups of microwave cavities [46] are experimentally tractable nowadays [91]. Input powers of the order of  $\sim$ kW yield corresponding ac fields of  $\sim 10$  kV/cm. This is already highly sufficient for what is needed for alkali dipolar molecules (see Table in Ref. [48]). The microwave energies available are in the range [2–18 GHz] which also correspond well to the energies needed (twice the rotational constant of the alkali dipolar molecules, see Table in Ref. [48]). Finally, although imperfect polarization could reduce the efficiency of the shielding, better experimental control over circular polarization becomes possible nowadays [92]. Therefore, with the current improvement of the microwave technologies, the control of the scattering length of dipolar molecules seems experimentally realistic, and will certainly open a new regime of strongly interacting and correlated physics with ultracold dipolar molecules.

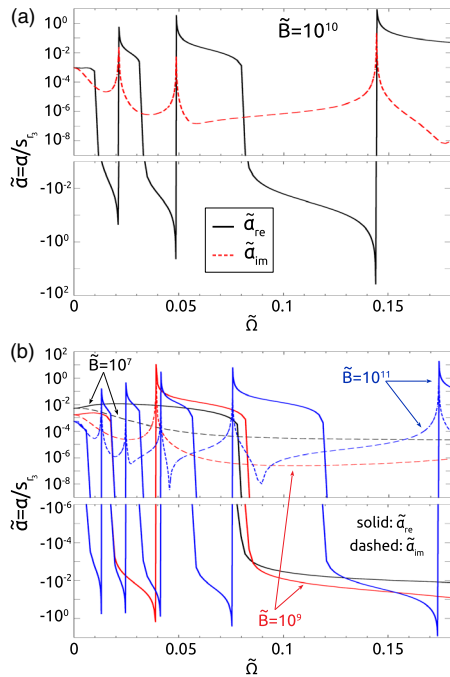


FIG. 4. (a) Top panel: Rescaled scattering length  $\tilde{a}$  as a function of  $\tilde{\Omega}$  for  $\tilde{B} = 10^{10}$  ( $\sim$ NaRb). (b) Bottom panel: Same for  $\tilde{B} = 10^7$  ( $\sim$ KRb),  $\tilde{B} = 10^9$  ( $\sim$ NaK, KCs),  $\tilde{B} = 10^{11}$  ( $\sim$ NaCs).



We acknowledge funding from the FEW2MANY-SHIELD Project No. ANR-17-CE30-0015, the COPOMOL Project No. ANR-13-IS04-0004 and the BLUESHIELD Project No. ANR-14-CE34-0006 from Agence Nationale de la Recherche. We also acknowledge fruitful and stimulating discussions with the Théomol team members, especially M. L. González-Martínez, A. Orbán, M. Lepers, O. Dulieu, and N. Bouloufa-Maafa.

- 
- [1] F. Dalfovo, S. Giorgini, L. P. Pitaevskii, and S. Stringari, *Rev. Mod. Phys.* **71**, 463 (1999).
- [2] A. J. Leggett, *Rev. Mod. Phys.* **73**, 307 (2001).
- [3] I. Bloch, J. Dalibard, and W. Zwerger, *Rev. Mod. Phys.* **80**, 885 (2008).
- [4] I. Bloch, J. Dalibard, and S. Nascimbène, *Nat. Phys.* **8**, 267 (2012).
- [5] C. A. Regal, M. Greiner, and D. S. Jin, *Phys. Rev. Lett.* **92**, 040403 (2004).
- [6] M. Bartenstein, A. Altmeyer, S. Riedl, S. Jochim, C. Chin, J. H. Denschlag, and R. Grimm, *Phys. Rev. Lett.* **92**, 120401 (2004).
- [7] M. W. Zwierlein, C. A. Stan, C. H. Schunck, S. M. F. Raupach, A. J. Kerman, and W. Ketterle, *Phys. Rev. Lett.* **92**, 120403 (2004).
- [8] T. Bourdel, L. Khaykovich, J. Cubizolles, J. Zhang, F. Chevy, M. Teichmann, L. Tarruell, S. J. J. M. F. Kokkelmans, and C. Salomon, *Phys. Rev. Lett.* **93**, 050401 (2004).
- [9] E. Braaten and H.-W. Hammer, *Phys. Rep.* **428**, 259 (2006).
- [10] V. Efimov, *Phys. Lett. B* **33**, 563 (1970).
- [11] T. Kraemer, M. Mark, P. Waldburger, D. J. G., C. Chin, B. Engeser, A. D. Lange, K. Pilch, A. Jaakkola, H.-C. Nägerl, and R. Grimm, *Nature (London)* **440**, 315 (2006).
- [12] D. Jaksch and P. Zoller, *Ann. Phys. (Amsterdam)* **315**, 52 (2005).
- [13] M. A. Baranov, M. Dalmonte, G. Pupillo, and P. Zoller, *Chem. Rev.* **112**, 5012 (2012).
- [14] H. Feshbach, *Ann. Phys. (N.Y.)* **5**, 357 (1958).
- [15] U. Fano, *Phys. Rev.* **124**, 1866 (1961).
- [16] E. Tiesinga, B. J. Verhaar, and H. T. C. Stoof, *Phys. Rev. A* **47**, 4114 (1993).
- [17] P. Courteille, R. S. Freeland, D. J. Heinzen, F. A. van Abeelen, and B. J. Verhaar, *Phys. Rev. Lett.* **81**, 69 (1998).
- [18] S. Inouye, M. R. Andrews, J. Stenger, H.-J. Miesner, D. M. Stamper-Kurn, and W. Ketterle, *Nature (London)* **392**, 151 (1998).
- [19] C. Chin, R. Grimm, P. Julienne, and E. Tiesinga, *Rev. Mod. Phys.* **82**, 1225 (2010).
- [20] M. Yan, B. J. DeSalvo, B. Ramachandran, H. Pu, and T. C. Killian, *Phys. Rev. Lett.* **110**, 123201 (2013).
- [21] T. L. Nicholson, S. Blatt, B. J. Bloom, J. R. Williams, J. W. Thomsen, J. Ye, and P. S. Julienne, *Phys. Rev. A* **92**, 022709 (2015).
- [22] K.-K. Ni, S. Ospelkaus, M. H. G. de Miranda, A. Pe'er, B. Neyenhuis, J. J. Zirbel, S. Kotochigova, P. S. Julienne, D. S. Jin, and J. Ye, *Science* **322**, 231 (2008).
- [23] K. Aikawa, D. Akamatsu, M. Hayashi, K. Oasa, J. Kobayashi, P. Naidon, T. Kishimoto, M. Ueda, and S. Inouye, *Phys. Rev. Lett.* **105**, 203001 (2010).
- [24] T. Takekoshi, L. Reichsöllner, A. Schindewolf, J. M. Hutson, C. R. Le Sueur, O. Dulieu, F. Ferlaino, R. Grimm, and H.-C. Nägerl, *Phys. Rev. Lett.* **113**, 205301 (2014).
- [25] P. K. Molony, P. D. Gregory, Z. Ji, B. Lu, M. P. Köppinger, C. R. Le Sueur, C. L. Blackley, J. M. Hutson, and S. L. Cornish, *Phys. Rev. Lett.* **113**, 255301 (2014).
- [26] J. W. Park, S. A. Will, and M. W. Zwierlein, *Phys. Rev. Lett.* **114**, 205302 (2015).
- [27] M. Guo, B. Zhu, B. Lu, X. Ye, F. Wang, R. Vexiau, N. Bouloufa-Maafa, G. Quéméner, O. Dulieu, and D. Wang, *Phys. Rev. Lett.* **116**, 205303 (2016).
- [28] T. M. Rvachov, H. Son, A. T. Sommer, S. Ebadi, J. J. Park, M. W. Zwierlein, W. Ketterle, and A. O. Jamison, *Phys. Rev. Lett.* **119**, 143001 (2017).
- [29] M. Mayle, B. P. Ruzic, and J. L. Bohn, *Phys. Rev. A* **85**, 062712 (2012).
- [30] M. Mayle, G. Quéméner, B. P. Ruzic, and J. L. Bohn, *Phys. Rev. A* **87**, 012709 (2013).
- [31] X. Ye, M. Guo, M. L. González-Martínez, G. Quéméner, and D. Wang, *Sci. Adv.* **4**, eaaq0083 (2018).
- [32] N. Balakrishnan, V. Kharchenko, R. Forrey, and A. Dalgarno, *Chem. Phys. Lett.* **280**, 5 (1997).
- [33] J. M. Hutson, *New J. Phys.* **9**, 152 (2007).
- [34] K.-A. Suominen, M. J. Holland, K. Burnett, and P. Julienne, *Phys. Rev. A* **51**, 1446 (1995).
- [35] K.-A. Suominen, *J. Phys. B* **29**, 5981 (1996).
- [36] R. Napolitano, J. Weiner, and P. S. Julienne, *Phys. Rev. A* **55**, 1191 (1997).
- [37] J. Weiner, V. S. Bagnato, S. Zilio, and P. S. Julienne, *Rev. Mod. Phys.* **71**, 1 (1999).
- [38] A. Micheli, G. Pupillo, H. P. Büchler, and P. Zoller, *Phys. Rev. A* **76**, 043604 (2007).
- [39] A. V. Gorshkov, P. Rabl, G. Pupillo, A. Micheli, P. Zoller, M. D. Lukin, and H. P. Büchler, *Phys. Rev. Lett.* **101**, 073201 (2008).
- [40] T. Karman and J. M. Hutson, preceding Letter, *Phys. Rev. Lett.* **121**, 163401 (2018).
- [41] G. Quéméner, in *Cold Chemistry: Molecular Scattering and Reactivity Near Absolute Zero*, edited by O. Dulieu and A. Osterwalder (The Royal Society of Chemistry, London, 2018), Chap. 12.
- [42] G. Wang and G. Quéméner, *New J. Phys.* **17**, 035015 (2015).
- [43] M. L. González-Martínez, J. L. Bohn, and G. Quéméner, *Phys. Rev. A* **96**, 032718 (2017).
- [44] S. Ospelkaus, K.-K. Ni, D. Wang, M. H. G. de Miranda, B. Neyenhuis, G. Quéméner, P. S. Julienne, J. L. Bohn, D. S. Jin, and J. Ye, *Science* **327**, 853 (2010).
- [45] K.-K. Ni, S. Ospelkaus, D. Wang, G. Quéméner, B. Neyenhuis, M. H. G. de Miranda, J. L. Bohn, D. S. Jin, and J. Ye, *Nature (London)* **464**, 1324 (2010).
- [46] D. DeMille, D. R. Glenn, and J. Petricka, *Eur. Phys. J. D* **31**, 375 (2004).
- [47] S. V. Alyabyshev and R. V. Krems, *Phys. Rev. A* **80**, 033419 (2009).
- [48] See Supplemental Material at <http://link.aps.org/supplemental/10.1103/PhysRevLett.121.163402> for the description of the effect of the electronic and nuclear spin structure and a magnetic field, the effect of the blue-detuned

- microwave radiation on the trapping of the molecules, the characteristic times of the problem and for a table of relevant parameters for different molecules, which includes Refs. [49–74].
- [49] J. Aldegunde, B. A. Rivington, P. S. Zuchowski, and J. M. Hutson, *Phys. Rev. A* **78**, 033434 (2008).
- [50] J. Aldegunde and J. M. Hutson, *Phys. Rev. A* **96**, 042506 (2017).
- [51] J. Aldegunde and J. M. Hutson, *Phys. Rev. A* **79**, 013401 (2009).
- [52] J. Aldegunde and J. M. Hutson, *Phys. Rev. A* **97**, 042505 (2018).
- [53] C. Cohen-Tannoudji, J. Dupont-Roc, and G. Grynberg, *Atom-Photon Interactions: Basic Processes and Applications* (Wiley-VCH, New York, 2008).
- [54] F. Reif, *Fundamentals of Statistical and Thermal Physics* (Waveland Press, Long Grove, IL, 2009).
- [55] Z. Idziaszek and P. S. Julienne, *Phys. Rev. Lett.* **104**, 113202 (2010).
- [56] N. Vanhaecke and O. Dulieu, *Mol. Phys.* **105**, 1723 (2010).
- [57] P. S. Zuchowski, M. Kosicki, M. Kodrycka, and P. Soldán, *Phys. Rev. A* **87**, 022706 (2013).
- [58] J. N. Byrd, J. A. Montgomery, and R. Côté, *Phys. Rev. A* **86**, 032711 (2012).
- [59] J. Chen and T. C. Steimle, *J. Chem. Phys.* **128**, 144312 (2008).
- [60] P. S. Zuchowski, J. Aldegunde, and J. M. Hutson, *Phys. Rev. Lett.* **105**, 153201 (2010).
- [61] R. Guérout, M. Aymar, and O. Dulieu, *Phys. Rev. A* **82**, 042508 (2010).
- [62] T. C. Steimle, P. J. Dommelle, and D. O. Harris, *J. Mol. Spectrosc.* **68**, 134 (1977).
- [63] W. Ernst, J. Kändler, S. Kindt, and T. Törring, *Chem. Phys. Lett.* **113**, 351 (1985).
- [64] C. Ryzlewicz and T. Törring, *Chem. Phys.* **51**, 329 (1980).
- [65] W. E. Ernst, J. Kändler, and T. Törring, *J. Chem. Phys.* **84**, 4769 (1986).
- [66] A. Bernard and R. Gravina, *Astrophys. J. Suppl. Ser.* **52**, 443 (1983).
- [67] R. D. Suenram, F. J. Lovas, G. T. Fraser, and K. Matsumura, *J. Chem. Phys.* **92**, 4724 (1990).
- [68] W. J. Childs, L. S. Goodman, U. Nielsen, and V. Pfeufer, *J. Chem. Phys.* **80**, 2283 (1984).
- [69] L. A. Kaledin, J. C. Bloch, M. C. McCarthy, and R. W. Field, *J. Mol. Spectrosc.* **197**, 289 (1999).
- [70] T. C. Steimle, D. A. Fletcher, K. Y. Jung, and C. T. Scurlock, *J. Chem. Phys.* **96**, 2556 (1992).
- [71] D. A. Fletcher, M. A. Anderson, W. L. Barclay Jr., and L. M. Ziurys, *J. Chem. Phys.* **102**, 4334 (1995).
- [72] Q. Shao, L. Deng, X. Xing, D. Gou, X. Kuang, and H. Li, *J. Phys. Chem. A* **121**, 2187 (2017), pMID: 28230993.
- [73] T. C. Steimle, J. Gengler, and J. Chen, *Can. J. Chem.* **82**, 779 (2004).
- [74] C. Ryzlewicz, H.-U. Schütze-Pahlmann, J. Hoeft, and T. Törring, *Chem. Phys.* **71**, 389 (1982).
- [75] B. Gao, *Phys. Rev. Lett.* **105**, 263203 (2010).
- [76] E. B. Norrgard, D. J. McCarron, M. H. Steinecker, M. R. Tarbutt, and D. DeMille, *Phys. Rev. Lett.* **116**, 063004 (2016).
- [77] S. Truppe, H. J. Williams, M. Hambach, L. Caldwell, N. J. Fitch, E. A. Hinds, B. E. Sauer, and M. R. Tarbutt, *Nat. Phys.* **13**, 1173 (2017).
- [78] L. Anderegg, B. L. Augenbraun, E. Chae, B. Hemmerling, N. R. Hutzler, A. Ravi, A. Collopy, J. Ye, W. Ketterle, and J. M. Doyle, *Phys. Rev. Lett.* **119**, 103201 (2017).
- [79] L. Anderegg, B. L. Augenbraun, Y. Bao, S. Burchesky, L. W. Cheuk, W. Ketterle, and J. M. Doyle, *Nat. Phys.* **14**, 890 (2018).
- [80] I. Kozyryev, L. Baum, K. Matsuda, B. L. Augenbraun, L. Anderegg, A. P. Sedlack, and J. M. Doyle, *Phys. Rev. Lett.* **118**, 173201 (2017).
- [81] M. T. Hummon, M. Yeo, B. K. Stuhl, A. L. Collopy, Y. Xia, and J. Ye, *Phys. Rev. Lett.* **110**, 143001 (2013).
- [82] J. D. Weinstein, R. deCarvalho, T. Guillet, B. Friedrich, and J. M. Doyle, *Nature (London)* **395**, 148 (1998).
- [83] B. Pasquiou, A. Bayerle, S. M. Tzanova, S. Stellmer, J. Szczepkowski, M. Parigger, R. Grimm, and F. Schreck, *Phys. Rev. A* **88**, 023601 (2013).
- [84] T. Chen, W. Bu, and B. Yan, *Phys. Rev. A* **94**, 063415 (2016).
- [85] A. Guttridge, S. A. Hopkins, M. D. Frye, J. J. McFerran, J. M. Hutson, and S. L. Cornish, *Phys. Rev. A* **97**, 063414 (2018).
- [86] A. Guttridge, M. D. Frye, B. C. Yang, J. M. Hutson, and S. L. Cornish, *Phys. Rev. A* **98**, 022707 (2018).
- [87] F. Munchow, C. Bruni, M. Madalinski, and A. Gorlitz, *Phys. Chem. Chem. Phys.* **13**, 18734 (2011).
- [88] A. Cournol, P. Pillet, H. Lignier, and D. Comparat, *Phys. Rev. A* **97**, 031401(R) (2018).
- [89] A. V. Avdeenkov and J. L. Bohn, *Phys. Rev. Lett.* **90**, 043006 (2003).
- [90] A. V. Avdeenkov, D. C. E. Bortolotti, and J. L. Bohn, *Phys. Rev. A* **69**, 012710 (2004).
- [91] D. P. Dunseith, S. Truppe, R. J. Hendricks, B. E. Sauer, E. A. Hinds, and M. R. Tarbutt, *J. Phys. B* **48**, 045001 (2015).
- [92] A. Signoles, E. K. Dietsche, A. Facon, D. Grosso, S. Haroche, J. M. Raimond, M. Brune, and S. Gleyzes, *Phys. Rev. Lett.* **118**, 253603 (2017).